

Fiske steps in annular Josephson junctions with trapped flux quanta

C. Nappi and R. Cristiano

Istituto di Cibernetica del Consiglio Nazionale delle Ricerche, Via Toiano 6, I-80072, Arco Felice, Napoli, Italy

M. P. Lisitskii

*Istituto di Cibernetica del Consiglio Nazionale delle Ricerche, Via Toiano 6, I-80072, Arco Felice, Napoli, Italy
and Institute of Radio Engineering & Electronics of the Russian Academy of Science, Mokhovaya str. 11, GSP-3, 103907,
Moscow, Russia*

(Received 20 January 1998; revised manuscript received 15 July 1998)

The position and amplitude of self-resonances (Fiske steps) of an annular Josephson junction with magnetic flux trapped in one of two electrodes have been calculated using a first-order perturbation method. The external magnetic field is supposed to be zero such that the only magnetic field to be considered is that provided by the flux quanta trapped in the junction annular electrodes during the cooling transition. Our analysis is carried out for the two-dimensional case so that the finite width of the ring tunnel barrier is taken into account. We find that in such a structure, although a two-dimensional one, a simply infinite series of modes is excited. We discuss the dependence of the amplitude and the position of the resonances on the ratio of the inner to outer radius of the junction, and we show that only the first Fiske step has a significant amplitude. The agreement between the predictions of the theory and the existing experimental data is very good.

[S0163-1829(98)08341-6]

I. INTRODUCTION

Annular Josephson tunnel junctions have received continuous attention in the course of the last two decades because of the particularly attractive phenomenology connected with them.¹⁻⁸ Investigations of the soliton propagation can be carried out in the absence of disturbing boundary reflections exclusively in the annular geometry. Annular junctions also have the unique property that fluxons (magnetic fluxoid quanta) can be permanently trapped in the junction barrier during the cooling process due to the topologically nonconnected geometry of one or both the electrodes. This leads, for example, to the nucleation of soliton-antisoliton pairs when a parallel magnetic field is present in the plane of the junction barrier and to a number of interesting related phenomena.

The term *annular* has been reserved in the literature to a geometry in which the width of the ring is small in comparison with the ring radius and the circumference of the ring is long in comparison with the Josephson penetration depth λ_j . In this case, it is possible to reduce the investigation of the junction electrostatics to a one-dimensional (1D) problem. On the other hand, when n fluxons have been trapped and the circumference L of the junction is, roughly speaking, smaller than $2n\lambda_j$, the trapped fluxons do not localize. In this case, if no external magnetic field is present, a simple configuration with cylindrical symmetry sets in.

Recently, the static and dynamics properties of annular junctions in the presence of a uniform magnetic field applied parallel to the junction plane have been investigated in Refs. 5-7. The analysis carried out in those works allows for the presence of trapped fluxons in the junction barrier through the hole of the primary electrode. However, the presence of a uniform barrier-parallel magnetic field shades the underlying cylindrical symmetry and does not permit full appreciation

of the peculiar phenomenology exhibited by this configuration.

In this paper we focus our attention on the problem of an annular Josephson tunnel junction in the presence of centrally trapped fluxons and in zero external field. We consider junctions for which $L \leq 2n\lambda_j$, unless otherwise specified, and *treat them fully two dimensionally*. After the fluxons have been trapped, during the cooling transition, the resulting configuration (see Fig. 1) has an especially simple character. The magnetic field lines are radially directed and uniformly spread all around the junction circumference with a good approximation. At the same time the magnetic flux can take on only values which are integer multiples of $\Phi_0 = h/2e$. This highly symmetric configuration, as well as the presence of trapped fluxons in itself, has a remarkable influence over the static and dynamic behavior of the junction. For example, the Josephson critical current may be completely suppressed under these conditions.^{5,6,9,10} The self-resonance properties of the junction (Fiske steps) should also undergo important changes, which is the subject of this paper.

It is well known that Fiske steps are excited in the junction cavity as a result of the interaction between the Josephson current and the electromagnetic fields.¹¹⁻¹³ The resonances appear in the zero-frequency current-voltage (I - V) characteristic at certain fixed voltages, which depend on the junction geometry, and their amplitude is modulated by the magnetic field intensity. In a previous paper,¹⁴ on the basis of a simplified analysis, two of the present authors pointed out the very symmetric self-resonance properties which an electrically small annular junction with trapped fluxons should exhibit in a zero external magnetic field.

We reconsider here in full detail the problem of the determination of the positions and amplitudes of the Fiske resonances, by using a first-order perturbation method. The sim-

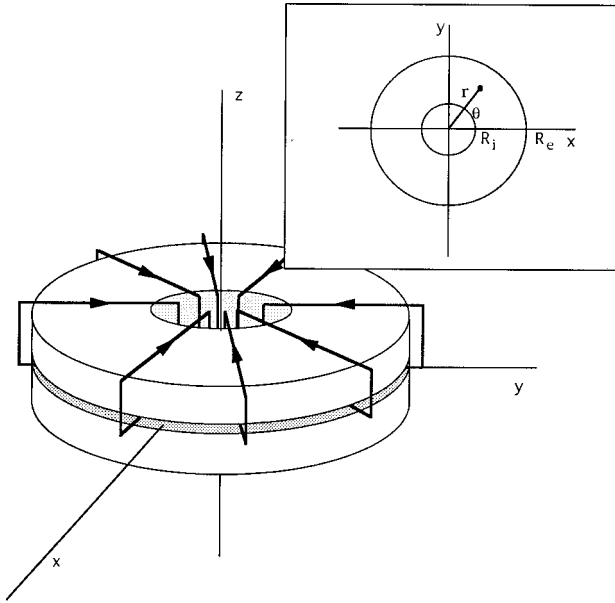


FIG. 1. Schematic of an annular Josephson junction with flux trapped in the top electrode. Shown are the magnetic field lines threading the electrode. Also shown is the coordinate system used.

plifying hypothesis of a vanishing ring width, which was implicit in Ref. 14, will be dropped in this paper. Our analysis reproduces the results of Nerenberg and Blackburn¹⁵ (as far as the *positions* of the Fiske resonances are concerned) for the case of a circular junction when the inner radius of the ring vanishes. On the other hand, we find, even for a finite junction width, a very peculiar amplitude distribution of the steps which reflects both the high degree of symmetry of the configuration (zero uniform external field) and the fluxoid quantization requirement. We give a complete discussion of these two main topics and some quantitative estimates of the appropriate model parameters. Finally, we compare the predictions of the theory with the experimental results reported by Vernik *et al.*⁸ on annular junctions with trapped fluxons. We show that our model accounts quantitatively for all the significant observed experimental features.

II. THEORY OF THE 2D ANNULAR CAVITY

Let us consider an annular junction, made of two identical superconductors, with n trapped fluxons as sketched in Fig. 1. The internal and external radius of the junction are denoted by R_i and R_e , respectively. We will assume that the electrode thickness is larger than the London penetration depth λ_L . The circumference of the junction, $2\pi R_e$, is assumed to be shorter than $2n\lambda_j$, where $\lambda_j = (\hbar/2\mu_0 e j_1 d)^{1/2}$ is the Josephson penetration depth (a fluxon can be considered $2\lambda_j$ ‘‘long’’). The symbols j_1 and d denote the maximum Josephson current density and the effective magnetic thickness $d = 2\lambda_L + s$, respectively, and s is the tunnel barrier thickness. In this case the magnetic field in the barrier can be considered, to a good approximation, radial and uniformly distributed all around the circular junction edge. Moreover, the flux threading the barrier is quantized and can be written as $\Phi = n\Phi_0$, where $n = 1, 2, \dots$ is the number of the trapped flux quanta. The invariant-gauge phase difference φ between

the two superconducting junction electrodes satisfies the Josephson equations

$$\nabla\varphi = (2\pi\mu_0 d/\Phi_0)\mathbf{H} \times \mathbf{u}_z \quad (1)$$

and

$$\partial\varphi/\partial t = 2eV/\hbar, \quad (2)$$

with \mathbf{u}_z a unit vector normal to the junction plane, V the total barrier voltage, both ac and dc, and \mathbf{H} the magnetic field. In the case of n flux quanta trapped through the central hole of the annular junction in the primary electrode, the magnetic field in the plane of the barrier has in a first approximation only a radial component, which can be easily calculated. At distance r , the magnetic field crosses a surface $2\pi r d$. Thus, if the screening effect of the Josephson current is neglected ($\lambda_j \rightarrow \infty$), the magnetic field of n trapped flux quanta is given by

$$H_n = n\Phi_0/(2\pi r\mu_0 d). \quad (3)$$

Equation (3) can be used in Eq. (1) for the field \mathbf{H} . In cylindrical-polar coordinates (r, θ) , this results simply in

$$\frac{\partial\varphi}{\partial r} = 0, \quad (4)$$

$$\frac{\partial\varphi}{\partial\theta} = -n. \quad (5)$$

Then Eqs. (2), (4), and (5) give a zero-order (no self-fields) invariant-gauge phase difference between the two electrodes as⁹

$$\varphi = \omega t - n\theta + \text{const}, \quad (6)$$

where $\omega = 2\pi V_0/\Phi_0$ is the Josephson frequency and V_0 the dc part of the total voltage. We refer to Eq. (6) as the ‘‘linear phase-difference approximation.’’ The better the condition $L < 2n\lambda_j$ is satisfied, the closer Eq. (6) represents the true phase difference between the electrodes.

A. Basic equations

The calculation of the Fiske step amplitudes can be carried out on the basis of a first-order perturbative calculation scheme.^{11,12} We shall take, from Eq. (6), for the lowest-order approximation $\varphi \approx (\omega t - n\theta)$ (the constant has been arbitrarily chosen zero), and then we shall introduce the small additive correction $|\varphi_1(r, \theta, t)| \ll 1$ to improve the solution: that is,

$$\varphi \approx \omega t - n\theta + \varphi_1(r, \theta, t). \quad (7)$$

The partial differential equation governing $\varphi_1(r, \theta, t)$ or, which is the same, the self-induced perturbation voltage $v = (\Phi_0/2\pi)\partial\varphi_1/\partial t$, $V = V_0 + v$ was given by Eck *et al.*¹¹ and Kulik.¹² It may be expressed in polar coordinates as¹⁵

$$\begin{aligned} \frac{1}{r} \frac{\partial}{\partial r} \left(r \frac{\partial v}{\partial r} \right) + \frac{1}{r^2} \frac{\partial^2 v}{\partial \theta^2} - \frac{1}{c^2} \frac{\partial^2 v}{\partial t^2} \\ - \frac{\omega}{c^2 Q} \frac{\partial v}{\partial t} = \left(\frac{\Phi_0 \omega}{2\pi \lambda_j^2} \right) \cos(\omega t - n\theta), \end{aligned} \quad (8)$$

where the additive correction $\varphi_1(r, \theta, t)$ has been dropped in the argument of the cosine, which is the present approximation (step amplitudes much smaller than the maximum Josephson current, self-fields negligible). In Eq. (8), $\bar{c} = (s/\mu_0 \varepsilon d)^{1/2}$ is the Swihart velocity, ε is the dielectric constant of the barrier region, and Q is an adjustable loss parameter or the ‘‘quality factor’’ of the junction cavity. It is also interesting to point out that an energy feeding mechanism is naturally understood in the choice $\varphi \approx \omega t - n\theta$ on the right-hand side of Eq. (8).

Boundary conditions require periodicity with respect to θ and

$$\left. \frac{\partial v}{\partial r} \right|_{r=R_i, R_e} = 0, \quad (9)$$

which state the total reflection condition of the electromagnetic waves at the inner and outer boundaries.

B. Analytical solution

Solutions will be sought now in the form of normal modes of a ‘‘flat’’ cylindrical-toroidal cavity operating in the TM mode (at frequency ω), with no field variation in the z direction:

$$\begin{aligned} v(r, \theta, t) = & \sum_{k,m} \{ [J_k(\gamma_{km}r) + c_{km}N_k(\gamma_{km}r)] \\ & \times (A_{km}^{(1)} \cos k\theta + A_{km}^{(2)} \sin k\theta) \cos \omega t \\ & + [J_k(\gamma_{km}r) + c_{km}N_k(\gamma_{km}r)] \\ & \times (B_{km}^{(1)} \cos k\theta + B_{km}^{(2)} \sin k\theta) \sin \omega t \}, \quad (10) \end{aligned}$$

where J_k and N_k are the k th-order Bessel functions of the first and second kind, respectively,¹⁶ $R_i < r < R_e$. The sum over k runs from 0 to infinity, while m ranges from 1 to infinity. Then the boundary conditions at the inner and outer peripheries ($r = R_i, R_e$), Eq. (9), are accounted for by requiring

$$\begin{aligned} J'_k(\gamma_{km}R_e) + c_{km}N'_k(\gamma_{km}R_e) &= 0, \\ J'_k(\gamma_{km}R_i) + c_{km}N'_k(\gamma_{km}R_i) &= 0, \quad (11) \end{aligned}$$

where the primes indicate the derivative with respect to the argument.

Equations (11) are a transcendent system of equations for the unknowns γ_{km} and c_{km} . As shown hereafter, these equations determine the positions at which resonances will appear. In order to use a dimensionless notation, we denote ($X_{km} = \gamma_{km}R_e$, c_{km}) the m th root of Eq. (11) and introduce $\delta = R_i/R_e$, the ratio between the inner and outer radii of the junction. Then Eqs. (11) become

$$\begin{aligned} J'_k(X_{km}) + c_{km}N'_k(X_{km}) &= 0, \\ J'_k(X_{km}\delta) + c_{km}N'_k(X_{km}\delta) &= 0. \quad (12) \end{aligned}$$

When $\delta \rightarrow 0$, then $c_{km} \rightarrow 0$ and Eqs. (12) reduce to the simpler condition $J'_k(X_{km}) = 0$, which determines the position of the self-resonances in a small circular junction.¹⁵ The coefficients of the expansion in modes, Eq. (10), are determined by substituting this expansion into Eq. (8). For each m , with $k \neq n$, a particularly simple result is obtained:

$$A_{km}^{(1)} = A_{km}^{(2)} = B_{km}^{(1)} = B_{km}^{(2)} = 0. \quad (13)$$

For each m , with $k = n$ we get

$$A_{nm}^{(1)} = \left(\frac{\Phi_0 \bar{c}^2}{2\pi\lambda_j^2 \omega} \right) \left[\frac{(1 - \bar{c}^2 \gamma_{nm}^2 / \omega^2)}{(1 - \bar{c}^2 \gamma_{nm}^2 / \omega^2)^2 + (1/Q)^2} \right] a_{nm}, \quad (14)$$

$$A_{nm}^{(2)} = \left(\frac{\Phi_0 \bar{c}^2}{2\pi\lambda_j^2 \omega} \right) \left[\frac{1/Q}{(1 - \bar{c}^2 \gamma_{nm}^2 / \omega^2)^2 + (1/Q)^2} \right] a_{nm}, \quad (15)$$

where

$$\begin{aligned} a_{nm} = & R_e^2 g_{nm} / \left\{ \frac{R_e^2}{2} \left(1 - \frac{n^2}{\gamma_{nm}^2 R_e^2} \right) \right. \\ & \times [J_n(\gamma_{nm}R_e) + c_{nm}N_{nm}(\gamma_{nm}R_e)]^2 \\ & - \frac{R_i^2}{2} \left(1 - \frac{n^2}{\gamma_{nm}^2 R_i^2} \right) \\ & \left. \times [J_n(\gamma_{nm}R_i) + c_{nm}N_{nm}(\gamma_{nm}R_i)]^2 \right\} \quad (16) \end{aligned}$$

and g_{nm} are the following integrals:

$$g_{nm} = \int_{\delta}^1 y [J_n(X_{nm}y) + c_{nm}N_n(X_{nm}y)] dy. \quad (17)$$

Moreover,

$$\begin{aligned} B_{nm}^{(1)} &= -A_{nm}^{(2)}, \\ B_{nm}^{(2)} &= A_{nm}^{(1)}. \quad (18) \end{aligned}$$

Once all the coefficients $A_{km}^{(1)}$, $A_{km}^{(2)}$, $B_{km}^{(1)}$, and $B_{km}^{(2)}$ have been obtained, the expansion for $v(r, \theta, t)$ is fully determined. This expansion can be cast in the form ($R_i < r < R_e$)

$$\begin{aligned} v(r, \theta, t) = & \sum_{m=1}^{\infty} \{ J_n(\gamma_{nm}r) + c_{nm}N_n(\gamma_{nm}r) \} \\ & \times [A_{nm} \cos(\omega t - n\theta + \alpha_{nm})], \\ A_{nm} = & \sqrt{(A_{nm}^{(1)})^2 + (A_{nm}^{(2)})^2}, \\ \alpha_{nm} = & \tan^{-1} \left(\frac{A_{nm}^{(2)}}{A_{nm}^{(1)}} \right), \quad (19) \end{aligned}$$

which shows the ‘‘mixed’’ nature of such a wave: progressive in θ and stationary in r . We note explicitly that in the

presence of n vortices only the n th azimuthal mode is selected, while the remaining modes ($k \neq n$) have zero amplitude.

C. I - V characteristics of the resonances

With $v(r, \theta, t)$ fully determined, we are in position for calculating the I - V characteristics of the resonances. We start calculating the phase which can be written as

$$\varphi = \omega t - n\theta - \psi_0 + \frac{2e}{\hbar} \int^t v(t') dt', \quad (20)$$

where the phase constant ψ_0 has been introduced. Its value will be fixed by the maximization requirement for the

current.¹⁷ We shall adopt the same view of the authors in Refs. 15 and 17 and think of it as a necessary relative phase shift between the free-junction oscillations [$\approx \sin(\omega t - n\theta)$] and the effective self-field generation, which also occurs to lowest order at an angular frequency ω . The net Josephson current is given by $j = j_1 \sin(\varphi)$; this is frequency modulated and contains a nonzero dc (zero-frequency) term which we denote $\langle j \rangle$. The time-independent spatially averaged current density J_{dc} is just

$$J_{dc} = \frac{1}{\pi(R_e^2 - R_i^2)} \int_{R_i}^{R_e} \int_0^{2\pi} \langle j \rangle r d\theta dr. \quad (21)$$

The time-averaging procedure gives

$$\begin{aligned} \langle j \rangle = \langle j_1 \varphi_1 \cos \varphi_0 \rangle = & \left(\frac{e j_1}{\hbar \omega} \right) \sum_m \{ [J_n(\gamma_{nm} r) + c_{nm} N_n(\gamma_{nm} r)] [A_{nm}^{(1)} \cos n\theta + A_{nm}^{(2)} \sin n\theta] \sin(n\theta + \psi_0) \\ & - [J_n(\gamma_{nm} r) - c_{nm} N_n(\gamma_{nm} r)] [B_{nm}^{(1)} \cos n\theta + B_{nm}^{(2)} \sin n\theta] \cos(n\theta + \psi_0) \}. \end{aligned} \quad (22)$$

Integration over the space coordinates of the previous expression for $\langle j \rangle$ and Eqs. (18) leads to

$$J_{dc} = \left(\frac{e j_1}{\hbar \omega} \right) \left(\frac{2R_e^2}{R_e^2 - R_i^2} \right) \sum_m g_{nm} [A_{nm}^{(1)} \sin \psi_0 + A_{nm}^{(2)} \cos \psi_0]. \quad (23)$$

The last step is finding the maximum with respect to ψ_0 of J_{dc} as given in Eq. (23). This is easily done, and the results read

$$J_{dc} = \left(\frac{e j_1}{\hbar \omega} \right) \left(\frac{2R_e^2}{R_e^2 - R_i^2} \right) \sum_m g_{nm} \sqrt{(A_{nm}^{(1)})^2 + (A_{nm}^{(2)})^2}, \quad (24)$$

which corresponds to the optimal choice for ψ_0 as

$$\psi_0 = \tan^{-1} \left[\frac{\sum_m g_{nm} A_{nm}^{(1)}}{\sum_m g_{nm} A_{nm}^{(2)}} \right],$$

or substituting the expressions for $A_{nm}^{(1)}$ and $A_{nm}^{(2)}$ we find

$$\frac{J_{dc}}{j_1} = \left(\frac{R_e^2}{\lambda_j^2} \right) \left(\frac{1}{\eta^2} \right) \sum_m \frac{F_m(n, \delta)}{\sqrt{(1 - X_{nm}^2/\eta^2)^2 + \left(\frac{1}{Q} \right)^2}} = \left(\frac{R_e^2}{\lambda_j^2} \right) J^*, \quad (25)$$

where

$$F_m(n, \delta) = 2g_{nm}^2 / \left\{ (1 - \delta^2) \left[\left(1 - \frac{n^2}{X_{nm}^2} \right) [J_n(X_{nm}) + c_{nm} N_{nm}(X_{nm})]^2 - \delta^2 \left(1 - \frac{n^2}{(X_{nm}\delta)^2} \right) [J_n(X_{nm}\delta) + c_{nm} N_{nm}(X_{nm}\delta)]^2 \right] \right\}. \quad (26)$$

We have introduced the normalized voltage $\eta = \omega R_e / \bar{c}$ and the ‘‘simplified current’’ J^* as in Ref. 15. Equation (25) plus the expressions for $F_m(n, r)$ and g_{nm} constitute a complete solution of the problem.

At a fixed value of n , the number of trapped fluxons, Eq. (25), is essentially a sum of many resonance lines centered (apart for a small shift due to the losses) at dimensionless voltages $\eta = X_{nm}$, $m = 1, 2, 3, \dots$, where X_{nm} are solutions of Eq. (12) and n is fixed, we remark again, by the number of flux quanta present in the junction. The usual units are recovered through the formula

$$V_{nm} = X_{nm} (\bar{c} \Phi_0 / 2\pi R_e). \quad (27)$$

From Eq. (25) the maximum amplitude of the m th step is obtained to a very good approximation at $\eta = X_{nm}$. At this value the m th term of Eq. (25) takes the form

$$\frac{J_{n \max}^m}{j_1} = \left(\frac{R_e^2}{\lambda_j^2} \right) \frac{Q F_m(n, \delta)}{X_{nm}^2}. \quad (28)$$

Equation (28) is the central result of this work. It provides the amplitudes of the m th Fiske step for an assigned number

TABLE I. Positions of the first (X_{11}) and second (X_{12}) Fiske steps as a function of $\delta=R_i/R_e$, the inner to outer radius ratio of the junction when one ($n=1$) flux quantum is trapped.

δ	X_{11}	X_{12}
10^{-6}	1.841	5.331
1/7	1.766	5.024
1/5	1.705	4.960
1/3	1.540	5.273
0.5	1.354	6.564
0.7	1.182	10.591
0.9	1.053	31.446
0.99	1.005	
0.99999	1.0000	

of flux quanta trapped for arbitrary δ . When the width of the ring decreases ($\delta \rightarrow 1$), the amplitude of the first step tends to the limiting value $(J_{dc}/j_1)^{\max}=(R_e/\lambda_j)^2 Q/(4n^2)$, $F_1(n, \delta \rightarrow 1)=1/4$. It is also shown below that, in the same limit, Fiske steps of higher order (which are associated with the presence of standing waves between the inner and outer edges of the junction) move towards very high voltage.

III. DISCUSSION

In Tables I and II the positions of the first and second Fiske steps ($m=1,2$), as calculated from Eq. (12), are given for increasing inner hole radius ($\delta \rightarrow 1$). Table I shows the case of one flux quantum trapped, Table II the case of two quanta trapped. We see that $X_{11} \rightarrow 1.0$ and $X_{21} \rightarrow 2.0$, and in general we can expect $X_{n1} \rightarrow n$. This means that, in the limit of a vanishing ring width, resonances can appear at voltages $V_n=n(\bar{c}\Phi_0/2\pi R_e)$, which are the same positions of the Fiske steps of a square junction of length $W < \lambda_j$ in a parallel magnetic field when $2\pi R_e$ is substituted for $2W$.

The position of the second Fiske step (and necessarily higher-order steps) moves towards very high voltage as the inner radius increases. In a vanishing-width junction, only the first step is present at a finite voltage because only the azimuthal mode is possible.

On the other hand, even in the case in which many resonances are present at finite voltages, especially for $R_i \rightarrow 0$, the relative amplitudes of the steps following the first ($m=1$)

TABLE II. Positions of the first (X_{21}) and second (X_{22}) Fiske steps as a function of $\delta=R_i/R_e$, the inner to outer radius ratio of the junction when two ($n=2$) flux quanta are trapped.

δ	X_{21}	X_{22}
10^{-6}	3.054	6.706
1/7	3.048	6.633
1/5	3.034	6.494
1/3	2.932	6.270
0.5	2.681	7.062
0.7	2.362	10.798
0.9	2.106	31.500
0.99	2.010	
0.99999	2.0000	

TABLE III. Normalized amplitudes $[F_m(n, \delta)/2X_{nm}^2]$ of the first three Fiske steps for $n=1,2,3$ trapped flux quanta, for a junction with a vanishing inner radius ($R_i \rightarrow 0$).

$n \backslash m$	$F_m(n, \delta=0)/(2X_{nm}^2)$		
	1	2	3
1	6.9×10^{-2}	3.9×10^{-4}	3.4×10^{-5}
2	2.2×10^{-2}	5.1×10^{-4}	6.4×10^{-5}
3	1.1×10^{-2}	4.9×10^{-4}	7.6×10^{-5}

are very small. Table III, which gives the values of $F_m(n, \delta)/2X_{nm}^2$ as a function of (n, m) in the case $R_i=0$, shows clearly this behavior. This result is confirmed by looking at Table IV in which the same quantity of Table III is reported, but for the value of δ which is fixed there to 1/3. Subsequent Fiske steps are even smaller in amplitude for this case.

For fixed n , Fiske resonances start at $\eta=X_{nm}$, $m=1,2,3,\dots$. Furthermore, the amplitude of such resonances is a quickly decreasing function of the resonance order m . From the practical point of view, as n increases, only one peak is expected at larger and larger distance X_{n1} from the origin. For example, for a junction with inner radius $R_i \approx 0$, $X_{n1}=1.841, 3.054, 4.201, 5.317, 6.415$, and 7.501 , respectively, with $n=1,2,3,\dots$ trapped flux quanta. These correspond, for a junction with $R_e=50 \mu\text{m}$ and $\bar{c}=10^7 \text{m/s}$ to voltages of 121, 201, 253, 277, 351, 423, and 442 μV , respectively.

In a cylindrical junction with no center hole¹⁴ in a parallel uniform magnetic field, Fiske steps are predicted to appear at dimensionless voltages $\eta=X_{km}$, where X_{km} is the m th zero of $J'_k(x)$. Thus a doubly infinite series of resonances exists depending on the two integers k and m . Current step amplitudes at these voltages are modulated by the magnitude of the uniform external magnetic field in the plane of the junction, which can assume, of course, all possible continuous values.

In an annular junction, the positions of the possible resonances are predicted from Eq. (12) and depend on the choice of the two integer numbers. However, in the absence of an external magnetic field and with n trapped flux quanta, only the series with $k=n$ is selected. Within this series, even with a vanishing inner hole radius, only the first step has a significant amplitude. For a larger inner radius, the amplitude of the first step increases; at the same time, the distance (on the voltage axis) between the first and subsequent steps increases more and more. For example, a junction with $R_e=50 \mu\text{m}$,

TABLE IV. Normalized amplitudes $[F_m(n, \delta)/2X_{nm}^2]$ of the first three Fiske steps for $n=1,2,3$ trapped flux quanta for a junction with a finite inner to outer radius ratio ($\delta=R_i/R_e=1/3$).

$n \backslash m$	$F_m(n, \delta=1/3)/(2X_{nm}^2)$		
	1	2	3
1	1.04×10^{-1}	3.2×10^{-5}	1.01×10^{-7}
2	2.7×10^{-2}	2.4×10^{-4}	1.89×10^{-6}
3	1.2×10^{-2}	4.4×10^{-4}	1.08×10^{-5}

$R_i = 35 \mu\text{m}$, and $\bar{c} = 10^7 \text{ m/s}$ and one fluxon trapped exhibits the second step at $699 \mu\text{V}$, quite far from the first step, which should be located around $78 \mu\text{V}$.

IV. COMPARISON WITH EXPERIMENTS

We have compared the results of our theory with the experiments of Vernik *et al.* on annular junctions.⁸ These authors have studied the properties of an annular Nb/Al-AlO_x/Nb Josephson junction with various number of fluxons trapped in the tunnel barrier. The external radius R_e of the junction was $71 \mu\text{m}$, and the internal radius R_i was $61 \mu\text{m}$ ($\delta = R_i/R_e = 0.859$). The Josephson penetration depth λ_j was calculated to be approximately $50 \mu\text{m}$; hence, the length of the external circumference $2\pi R_e$ was about $8\lambda_j$.

After the trapping of a different numbers of fluxons, the authors of Ref. 8 measured both the dependence of the Josephson critical current I_c on the parallel magnetic field H and the I - V characteristic. The experimental I_c vs H dependences, obtained by these authors for various numbers n of trapped fluxons, are represented by closed dots in Fig. 2(a) ($n=0$), Fig. 2(b) ($n=2$), and Fig. 2(c) ($n=4$). We calculated the I_c vs H dependences, for the same number of trapped fluxons, by the following analytical formula which rests on a linear phase-difference approximation:⁹

$$\frac{I_c}{I_0} = \left| \frac{2}{(1-\delta^2)} \int_{\delta}^1 x J_n \left(x \frac{H}{H_0} \right) dx \right|_{(n=0,1,2,\dots)},$$

$$H_0 = \frac{\Phi_0}{2\pi R_e \mu_0 d}, \quad I_0 = j_1 \pi (R_e^2 - R_i^2). \quad (29)$$

We used the same value for the effective magnetic thickness d in all calculated theoretical dependences. This value of d ($d = 0.178 \mu\text{m}$) was defined as a fit parameter in the case of $n=0$. The results of the calculations obtained by Eq. (29) are shown in Figs. 2(a)–2(c) as solid lines. As can be seen from Fig. 2, good agreement is found between the experimental and theoretical I_c vs H patterns. Incidentally, this agreement is better than that found by the authors of Ref. 8. In fact, they used a simple form of Eq. (29) valid in the limit $R_i/R_e \rightarrow 1$ (in their case $R_i/R_e = 0.859$). This means that both the parameters of the junctions and the experimental conditions which were used in Ref. 8 match the main assumption of the theory described in Sec. II, i.e., the assumption of an essentially linear dependence for the invariant-gauge phase difference from the coordinates.

Now, in exact agreement with the prediction of our theory (see Sec. III), the authors of Ref. 8 found that, in the case of two trapped fluxons, the I - V characteristic in zero parallel magnetic field shows *only* the resonance branch ($n=2$, $m=1$), with a normalized maximal amplitude of 0.45 (Fig. 4 of Ref. 8). For the case of four trapped fluxons, *only* the resonance branch ($n=4$, $m=1$), with a normalized maximal amplitude of 0.23, was observed in the zero parallel magnetic field (see Fig. 5 of Ref. 8), so that the ratio between the experimental values of the maximal resonance branch amplitude at $n=2$ and $n=4$ was 1.95.

When a parallel magnetic field was applied, lower-order resonance branches manifest themselves as a consequence of the broken cylindrical symmetry. The voltage positions of

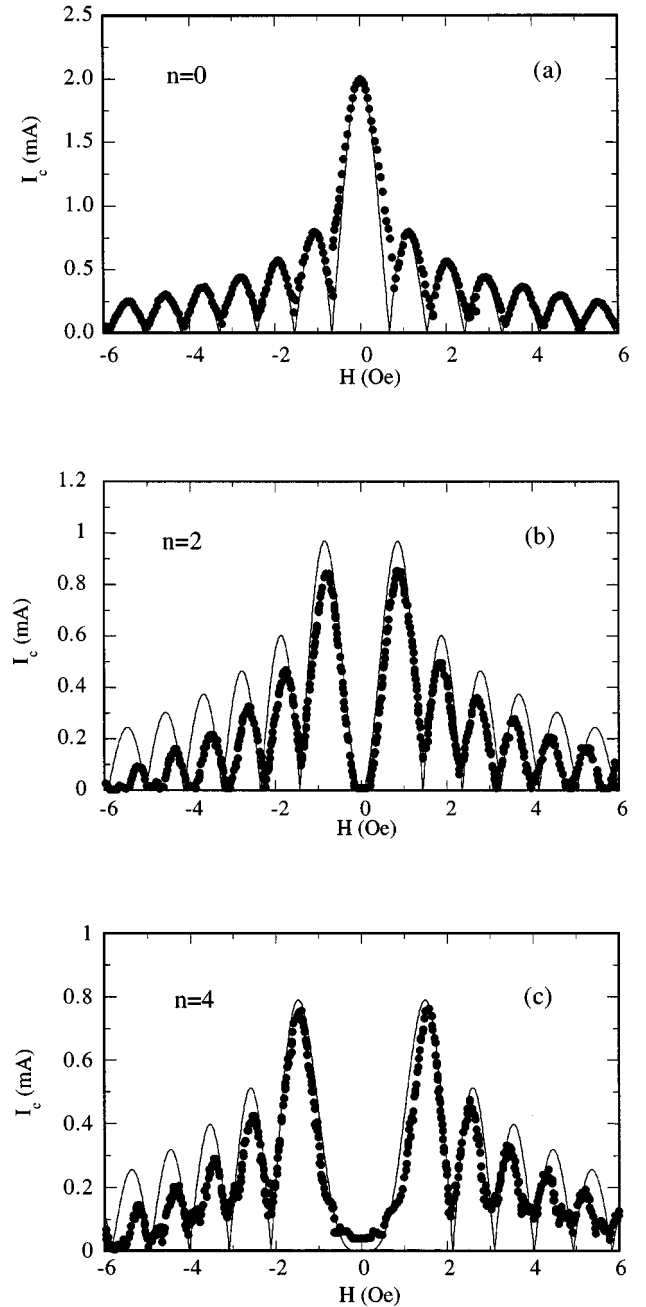


FIG. 2. Magnetic field H dependence of the critical current I_c with (a) no trapped fluxons, (b) two ($n=2$) trapped fluxons, and (c) four ($n=4$) trapped fluxons. The data points represent the experimental data of Vernik *et al.* (Ref. 8): the solid line shows the theoretical dependence given by Eq. (29).

the registered first, second, third, and fourth resonance steps were 50 , 100 , 150 , and $200 \mu\text{V}$, respectively.

Solving the system (12), with $\delta = 0.859$, we obtain $X_{11} = 1.08$, $X_{21} = 2.15$, $X_{31} = 3.23$, and $X_{41} = 4.30$. Substituting these values into Eq. (27), with a Swihart velocity $\bar{c} = 0.997 \times 10^7 \text{ m/s}$, we obtain for the theoretical voltage positions of resonance steps $V_{11} = 50.0 \mu\text{V}$, $V_{21} = 100.0 \mu\text{V}$, $V_{31} = 149.9 \mu\text{V}$, and $V_{41} = 199.9 \mu\text{V}$, which are in very good agreement with the experimental data. We are also in a position to account for the ratio between the amplitudes of the two steps at zero field. Using Eq. (28), we calculate

the ratio between the amplitudes of the resonances of the junction used in the experiments with $n=2$ and $n=4$ trapped vortices as $J_{2\max}^1/J_{4\max}^1=[F_1(2,0.859)X_{41}]/[F_1(4,0.859)X_{21}]\approx X_{41}/X_{21}=2.0$, which is also in excellent agreement with the observed experimental result.

Thus our theory (a fully 2D, analytical, improved treatment of the self-resonances in an annular junction) accounts for all the significant features obtained in the experiments of Ref. 8 with a quantitative agreement which can be considered very good. It is worth noticing that good agreement is obtained in spite of the condition $L < 2n\lambda_j$ not being verified for $n=2$. The point is that the condition $L < 2n\lambda_j$ (a purely geometrical one) is probably too severe for a linear phase-difference approximation (or some form of approximation equivalent to it) to be safely applied.

V. CONCLUSIONS

In conclusion, Fiske steps may be excited in an annular Josephson tunnel junction with trapped flux quanta and zero external field. In this case the necessary magnetic field is provided by the flux quanta themselves. The local value of the magnetic field is fixed by the condition that the flux across the barrier be an integral number of $\Phi_0=h/2e$. We have found expressions for the amplitudes and positions of

the Fiske steps of such a configuration, employing a simple perturbation technique. Our analysis takes into account the finite width of the annular junction barrier so that our results apply to annular junctions, with $L < 2n\lambda_j$, for an arbitrary electrode inner radius.

Current peaks are shown to occur at a discrete position depending on a single integer mode number m , once the number of flux quanta n in the junction has been fixed. With fixed n , the amplitude of the steps decreases quickly with the order of the steps. This allows us to state that this special configuration exhibits actually only one step with a significant amplitude. Moreover, as the hole radius reduces, the amplitude of the first Fiske step decreases. Higher-order steps appear at large voltages even for a small hole radius and then out of the range of any practical consideration as soon as the hole radius is made larger. We have tested the theory against the existing experimental results on annular junctions and obtained very good agreement.

ACKNOWLEDGMENTS

We wish to thank Professor I. Kulik for helpful discussions and comments on this subject while he was visiting our Institute. We also gratefully acknowledge discussions with M. Fistul'.

-
- ¹D. W. McLaughlin and A. C. Scott, Phys. Rev. A **18**, 1652 (1978).
- ²A. Davidson, B. Dueholm, and N. F. Pedersen, J. Appl. Phys. **60**, 1447 (1986).
- ³W. Wang, Q. Wang, and X. Yao, J. Appl. Phys. **70**, 6970 (1991).
- ⁴V. Vernik, N. Lazaridies, M. P. Sorensen, A. V. Ustinov, N. F. Pedersen, and V. A. Oboznov, J. Appl. Phys. **79**, 7854 (1996).
- ⁵N. Martucciello and R. Monaco, Phys. Rev. B **53**, 3471 (1996).
- ⁶N. Martucciello and R. Monaco, Phys. Rev. B **54**, 9050 (1996).
- ⁷N. Martucciello, C. Soriano, and R. Monaco, Phys. Rev. B **55**, 15 157 (1997).
- ⁸V. Vernik, S. Keil, N. Thyssen, T. Doderer, A. V. Ustinov, H. Kohlstedt, and R. P. Huebener, J. Appl. Phys. **81**, 1335 (1997).
- ⁹C. Nappi, Phys. Rev. B **55**, 82 (1997).
- ¹⁰A. A. Golubov and M. Y. Kupriyanov, Sov. Phys. JETP **65**, 849 (1987).
- ¹¹E. Eck, D. J. Scalapino, and B. N. Taylor, in *Proceedings of the 9th International Conference on Low Temperature Physics*, edited by J. G. Daunt (Plenum, New York, 1965), pp. 415–420.
- ¹²I. O. Kulik, Zh. Eksp. Teor. Fiz. Pisma Red. **2**, 134 (1965) [JETP Lett. **2**, 84 (1965)].
- ¹³A. Barone and G. Paternò, *Physics and Applications of the Josephson Effect* (Wiley, New York, 1982), Chap. 9.
- ¹⁴C. Nappi and R. Cristiano, Appl. Phys. Lett. **70**, 1320 (1997); R. Cristiano *et al.*, in *Proceedings of the 7th International Workshop on Low Temperature Detectors (LTD-7)*, edited by S. Cooper (Max Planck Institute of Physics, Munich, 1997), pp. 37–38.
- ¹⁵M. A. H. Nerenberg and J. A. Blackburn, Phys. Rev. B **9**, 3735 (1974).
- ¹⁶G. Arfken, *Mathematical Methods for Physicists* (Academic, Orlando, FL, 1985).
- ¹⁷J. A. Blackburn and M. A. H. Nerenberg, Phys. Lett. **46A**, 15 (1973).